Loss Dependence on Beam Position in the Arm Cavities of aLIGO

Leo Tsukada
supervised by
Denis Martynov and Valery Frolov

09/26/2014

ABSTRACT

High beam power in the interferometer is an essential component to realize required sensitivity to Gravitational waves. Therefore it is significant to understand main factors which cause optical loss in the arm cavities although we have not completely verified the effect of these factors on power loss. In this project we introduce the simulating model of the optical loss, called the clipping model, and investigate the loss dependence on beam off-centering on the test mass. An informative method which we adopt in the measurement makes it possible to derive not only optical loss but also other optical values. We also discuss some noise caused by Input Mode Cleaner in order to estimate accurate loss quantities. As a result, we confirm that the loss dependence appears to be consistent with the clipping model. However we cannot evaluate the agreement statistically between theory and practice because of the shortage of experimental data. Thus more data at various spots on the optics are required as a future work in order to make precise maps of the mirror with optical losses.

TABLE OF CONTENTS

1 Purpose and introduction

The basic method to detect GWs with an interferometric instrument is to observe the interference between two beams propagating through each arm cavity. It is because the interference signal shows differential length of the arm cavities, that is, the GWs effect on displacement of test masses. Large amplitude of the interference signal makes it possible to realize extremely high sensitivity to GWs and small optical loss during round trip in arm cavities is very important to keep the amplitude as large as possible. Therefore we need to understand main mechanism of optical round trip loss.

Although the actual loss results from multiple factors, broadly speaking, the main factors of round trip loss consist of geometric and scattering loss. [1] Geometric loss is caused by the beam intensity distribution which spreads out infinitely on the optics. It means that even if beam is placed on exactly the center of a mirror, since any mirror has a finite aperture, beam power leaks out more or less. Scattering loss results from the beam power reflected randomly from surface of optics toward outside of a cavity. The former factor is comparatively easy to simulate. The latter, on the other hand, is harder because the random surface roughness of the mirror is too complicated to simulate accurately. In this project we focus on only geometric factor and apply a specific model to the theory of geometric loss.

2 Simulation

The clipping model was adopted as a basic way to estimate the optical loss which is positioned off the center of the mirror. This model regards the beam which leaks out of the mirror as completely power loss. The total loss, therefore, is derived from the integral of the beam intensity distribution over the outside the mirror as a function of 'a', which is the distance between the centers of beam spot and the mirror. The loss function '$L(a)$' is defined as

$$L(a) = 1 - \frac{1}{N} \iint_D e^{-\frac{2}{w^2}\left((x-a)^2+y^2\right)} dxdy \quad st\, D : x^2 + y^2 \leq R^2 \tag{1}$$

$$N = \int_{-\infty}^{\infty} \int_{-\infty}^{\infty} e^{-\frac{2}{w^2}\left((x-a)^2+y^2\right)} dxdy = \frac{\pi w^2}{2} \tag{2}$$

where N is the normalization factor defined as (2), w is the beam spot size on the mirror and R is the radius of the mirror, which is technically the radius of mirror coating. In this model, any other higher-order spacial mode than the fundamental one (that is TEM_{00}) are ignored, which means that the intensity distribution approximates the Gaussian function. As shown in Fig.1, the off-centering Gaussian distribution is clipped over the blue circle which represents a mirror. The integral term in (1), which corresponds to clipped area in Fig.1, shows the total beam power on the mirror.

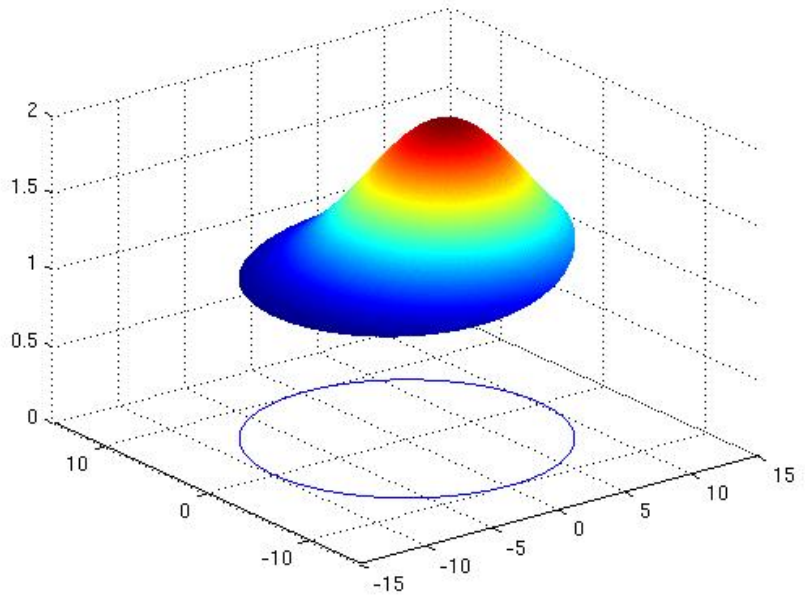

Fig 1: Schema of clipped Gaussian distribution. R is set to be 10 and a is 5 for simplicity.

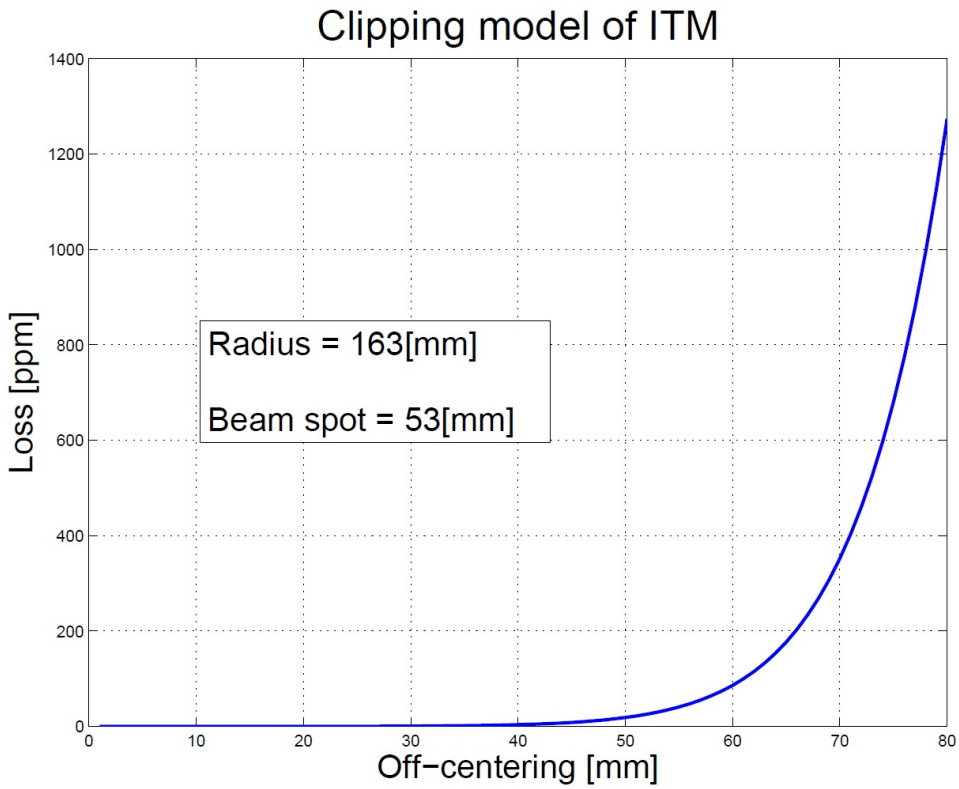

Fig 2: Clipping model of ITM. The radius of mirror coating and beam width on ITM are fixed to be reference as shown in the textbox. [1][2]

Fig 2 shows the simulated dependence of round trip loss on beam off-centering (a [mm]) at the given coating radius (R [mm]) and beam width (w [mm]), calculated by MATLAB based on (1). The optical loss increases exponentially as the beam position gets away from the center of ITM. It is explained in terms of the shape of Gaussian distribution, which means that the intensity around the maximum of Gaussan distribution is much larger than that of the foot. In other words, large a, extreme off-centering, makes beam power around the maximum leak and it causes huge loss in the arm cavities.

The other interesting point is that round trip loss is significantly small if beam position is within around 40 mm from the center. However it is not likely to happen in the actual experiment because the other loss factors such as scattering loss probably exceed geometric loss at that position. Therefore the experimental loss quantities at around the center of ITM will give us information to roughly estimate the effect of those factors.

3 Experiment

3.1 Outline

The measurement methodology is based on "Ringdown technique" of Tomoki Isogai's paper. [3] In this technique, the arm cavity was set to be two states, which are lock/non-lock states, and optical loss value was derived from the storage-time of the arm cavity. Although other experimental techniques to estimate optical loss are also known such as "Doppler technique", "Ringdown technique" has two advantages. First we can compute not only cavity round-trip loss but also the transmissivity of ITM, finesse of measured arm cavity and cavity mode-matching ratio. (See §3.4 for the detail.) Second it allows much less uncertainty of results than other methods. That great precision is probably caused by the non-resonance feature of this method. To put it in detail, the reflected power from the ITM of each arm cavity was measured by a photo detector (PDA100a, which is represented as PD in the following discussion). Firstly the PD signal was captured without the arm lock. Then the mirrors (PR2, IM4 and ITM/ETM of measured arm cavity) along the light path, as shown in Fig.3, were aligned by using "Initial alignment script" so that the reflected power from the ITM will go up to maximum. After completing the alignment, the cavity gets unlocked by using polarity switch in the fast path of the IMC board. The oscilloscope is supposed to measure the PD signal during that lock-loss. (See Fig.4) In the end, we analyze the data and derive a loss quantity from those signals in the two states.

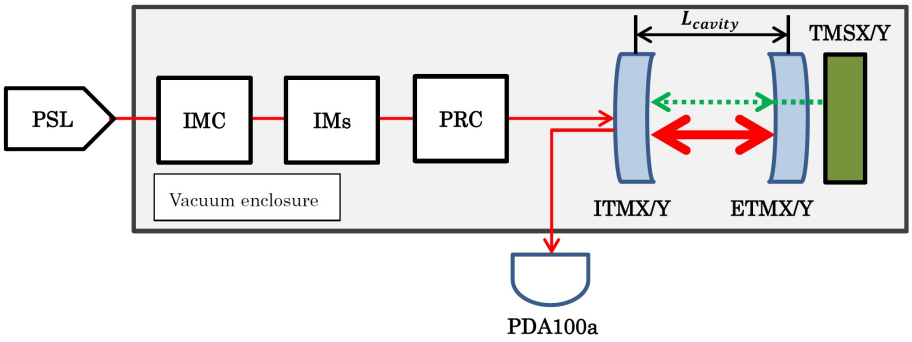

Fig 3: The schematic diagram of measurement. Some reports are needed to refer in detail for the configuration inside pre-stabilized laser (PSL), input mode cavity (IMC), input mirrors (IMs) and power recycling cavity (PRC). [2][4] The beam splitter (BS) is left out because BS basically has nothing to do with alignment in this measurement.

3.2 Experimental set-up

The basic layout of optics is the same as the full interferometer except that the schematic diagram above includes only one arm cavity since the loss measurement in each arm cavity is conducted separately. Take a close look at each optics along the

red light path. Firstly PSL is the servo system to stabilize the frequency and power of incident beam and is composed of some optical components such as a pockets cell (PC) and an acousto-optics modulator (AOM). [4] The stabilized beam propagates into the vacuum chamber and then IMC, which is supposed to filter out some laser noise so that the main carrier field and the modulation sideband fields will all pass through the IMC. Finally the beam reaches ITMX/Y via the four input mirrors and PMC. The input mirrors were aligned to expand the beam and couple it into the arm cavity mode. PMC amplifies the stored beam power efficiently by recycling the power loss in the Michaelson interferometer so that the power becomes resonant inside PMC. An input mirror, IM4, and a power recycling mirror, PR2, play an important role in finely adjusting the orientation of incident wave-front for arm cavity lock. More detail of each optics is shown in the overview report of aLIGO. [4] All sets of measurement were carried out while IMC was locked so that original and modulated beams would be resonant inside IMC. In the non-lock state where none of beam field matches with the arm cavity mode, the PD observes all the reflected power from ITMX/Y directly. In the lock state, on the other hand, it observes the resonant power transmitted from measured arm cavity along with non-coupled power. The analysis method for analysis is discussed more mathematically in the following section.

3.3 Initial alignment script

As noted above, we used programming script called "Initial alignment script" in adjusting alignment of some optics. The script makes it possible to place the beam on an arbitrary position of ITMX/Y unless the target position is extremely far away from the center of ITMX/Y. This flexibility is essential for this experiment since the purpose of this project is to verify the dependence of loss on the beam position on ITM. Therefore we needed to run the alignment script every time the beam position was changed. The alignment process of the initial alignment script is worth while to mention in order to understand our experimental results correctly. First of all, the PSL power is multiplied up to 9.5W and ITM/ETM are misaligned so that any beam will be completely scattered to outside of the arm cavity. Now let's call the stabilized beam, which we have discussed up to the previous section, "the red beam". In fact we employed another beam, called "the green beam", which is injected from the transmission monitor (TMSX/Y) located behind ETM in order to align ITM and ETM. TMSX/Y is aligned to fix the green beam on the target location, which was input manually onto the alignment script, on ITMX/Y. The actual beam position on ITMX/Y is sensed as a set of X and Y-coordinate [pc] by the camera mounted in front of each ITM. Therefore the script can be executed to sense the actual beam position and to run the ETM alignment actuator simultaneously in order to make the position as close as possible to the target. After completing TMSX/Y alignment, ITMX/Y is aligned by taking an average of the two sensed powers of baffle photo detectors (BPD) mounted on the edge of ETMX/Y so that "the green beam" reflected from ITM can be centered on ETMX/Y. This completion of ITM alignment can contribute to resonant condition inside the cavity. Then the script restores the pitch and yaw of ETM to the

reference values of previous locked alignment and the green beam (the red beam as well) reflected from ETM should be positioned at least within ITM again. Next thing to do is to make the red beam position approach the green one gradually by adjusting ETMX/Y alignment, where the power of green beam is no longer sensed by the ITM camera since the power of the red beam is much higher than that of the green beam. Finally the arm cavity alignment comes to an end when the red beam axis has been approximately superposed on the green axis and the green beam become resonant in the cavity. At this phase, the red beam is not necessarily resonant because IM4 and PR2 are also needed to finely adjust for perfect resonance, that is, the orientation of wave-front is required to match with the arm cavity mode. Therefore the script is supposed to run Wave Front Sensing (WFS) system, which aligns IM4 and PR2 so that the reflected power from ITM is maximum. After running the initial alignment script, the red beam is immediately extinguished by the polarity switch in the path of IMC board.

3.4 Measurement and analysis

Not only do we need to make measurements in non-lock state and lock state, but the measuring order is important to carry out the measurement efficiently and accurately. Here is the procedure of the measurement, which consists of four steps. (i)Set/change the target position which is supposed to be input onto the initial alignment script. (ii)Wait until IMC gets locked. (iii)Force the oscilloscope to apply a trigger to the PD signal (non-lock state). (iv)Run the initial alignment script (at given target point). (vi)Set the polarity switch to be off then arm-lock and IMC-lock will get lost. (v)Observe the PD signal during the lock-loss with the oscilloscope. The reason why the non-lock state has to be measured prior to lock state is that once the incident beam is blocked, not only the arm cavity but also IMC gets unlocked. These steps are circulated by several times and the set of the procedure is repeated at several different target positions. We experientially confirmed that the script could execute and complete cavity lock as long as the input location is within half of radius of ITM from the center.

Before moving on to analysis method, let me note the background theory in order to understand the analytic computation. First of all, we split the PD signal at the lock state into two time divisions called stable/relaxed division. Then let's define amplitude/power reflectivity of ITM (ETM) as $r_i(r_e)$ and $R_i(R_e)$ respectively and similarly amplitude/power transmissivity as $t_i(t_e)$ and $T_i(T_e)$ (where lower indexes i and e mean ITM and ETM). L_i and L_e are defined as normalized loss quantities of each test mass. Considering the reflected power from the cavity in the steady division, the reflected beam power can be written as

$$P_{refl} = P_0 K[r_i - r_e(T_i + R_i)]^2 + P_1 \tag{3}$$

where $P_0(P_1)$ is the coupled (uncoupled) component of incident beam power (apparently $P_{in} = P_0 + P_1$) into the fundamental cavity spatial mode, that is, TEM_{00}. K is the cavity gain defined as $[1/(1 - r_1 r_2)]^2$. [3] Since (3) describe optical quantities

at the steady division, this formula is independent of time transition t. If the beam gets blocked and nothing is incident into the cavity, that is, lock loss has happened, the PD signal changes from steady division into relaxed division. The beam which remains in the cavity is extinguished immediately while reflecting alternately from the two mirrors at countless times. Then this beam decay causes the reflected power to decreases exponentially as well. The time evolution of the reflected power can be written as

$$P_{refl}(t) = P_0 K T_i^2 R_e \, exp(-2t/\tau) \tag{4}$$

where t, time variable, is set to be $t = 0$ at the moment the beam gets blocked. τ is storage time of the arm cavity, defined as

$$\tau = \frac{2\,\ell\,F}{\pi\,c} \tag{5}$$

where ℓ and F are length and finesse of the cavity respectively. [3] Then finesse is given as

$$F = \frac{\pi\sqrt{r_i r_e}}{1 - r_i r_e} \tag{6}$$

Here consider the product of each tailer expansion of input/end mirror reflectivity. For $r_i = \sqrt{1 - L_i - T_i}$ and $r_e = \sqrt{1 - L_e - T_e}$, $r_i r_e$ approximates

$$\begin{aligned} r_i r_e &\simeq (1 - \frac{1}{2}(L_i + T_i))(1 - \frac{1}{2}(L_e + T_e)) && (7)\\ &\simeq 1 - \frac{1}{2}(L_i + L_e + T_i + T_e) && (8)\\ \Leftrightarrow L_i + L_e &= 2(1 - r_i r_e) - (T_i + T_e) && (9) \end{aligned}$$

Thinking about (3), (5),(6) and (9), the information about the round trip loss in the cavity can be extracted from the ringdown waveform written as (3).

The data analysis is conducted by computing a solution of a few equations with regards to each variables (P_0, P_1, r_i, t_i and r_e). According to Fig.4 below, each of the measurable value ($m_1 \sim m_4$) obtained from the PD signal of reflected power is determined as

$$\begin{aligned} m_1 &= P_0 + P_1 && (10)\\ m_2 &= P_0 K T_i^2 R_e && (11)\\ m_3 &= P_0 K [r_i - r_e(T_i + R_i)]^2 + P_1 \quad (See(3)) && (12)\\ m_4 &= \tau/2 && (13) \end{aligned}$$

where all four variables to derive (P_0, P_1, r_i, t_i and r_e) are contained. Although one degree of freedom still remains, we assumed $R_e = (1 - 5.0 \times 10^{-6})$ and $T_e = 5.0 \times 10^{-6}$. This simplification makes it possible to solve these equations uniquely. It means that the clipping loss cannot be applied only on ETM, because $L_e = \sqrt{1 - R_e - T_e} = 0$. Strictly speaking, the incident beam will be clipped twice by the both test masses

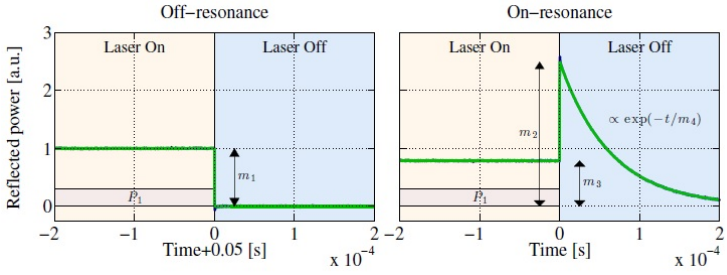

Fig 4: Signal sample of the reflected power. Off/On-resonance correspond to non-lock/lock state respectively. Pink and sky blue domains represent steady and relaxed division respectively.[3]

during a round trip, but this approximation is consistent with our experimental set-up. In this measurement, the clipping loss on ITM is significantly high compared to the loss on ETM because bottom TMSX/Y mirror is precisely coaligned with the center of ETMX/Y and the round trip loss on ETM can approximate zero at the beam position of less than around 40 mm from the center. (See Fig.2)

Additionally we move on to discussion about some noise caused by the ringdown speed of IMC. Since in principle the incident beam power is ideally assumed to vanish at the same time as lock loss, the time evolution of the reflected power on non-lock state appears to be step function as shown in Fig.4. In practice, however, IMC is also a kind of optical cavities and is similarly supposed to show ringdown waveform more or less as soon as lock loss. Although the time constant in IMC is considered to be generally much smaller than that of the arm cavity and to be negligible when analyzing the data, we need to reduce the effect of this noise on the loss quantities for more reliable conclusion. Therefore we measured the ringdown speed, that is, time constant of IMC in the similar way to "Ringdown technique". The transmitted power through IMC was observed during the lock loss and then we derived an exponential model function which would fit best into the observed wave form. (See appendix for detail) As a result, we obtained the time constant of 9.07[μs]with the standard error of 0.3%. This result appears convincing compared to the designed value, 9.13[μs], which is estimated based on the reference of optical properties of IMC. [4] In order to reduce the noise by IMC ringdown, we shortened the ringdwon waveform to fit into. As a result, the waveform from 20[μs] to 3000[μs] just after the lock loss was extracted. (See Fig.5)

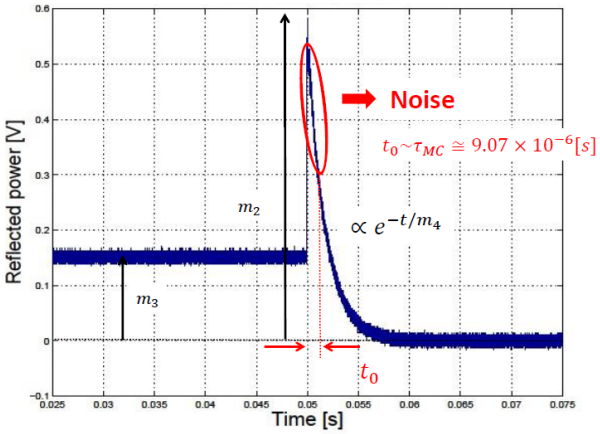

Fig 5: Schema of noise reduction

4 Results

4.1 Comparison between X-arm and Y-arm

In the cases of both arms, the target beam position on each ITM was stepped outward by 4 [pc] from the center up to the half of the radius, roughly 80 [mm]. Since the exact center position is not available, it was estimated by running another script which puts the beam on approximate center position by using BPDs on the edge of ETM. Additionally we calibrated the pixel of ITMX/Y cameras to physical distance on each ITM respectively. The results in each arm are shown in Fig.6, where the horizontal axis represents the distance of each beam position from the estimated center. Both of the red and blue plots show global-increasing dependence on the off-centering, although the plots increase and decrease locally. The measurement at the same beam position was conducted at basically twice or three times. Some data points which do not show any error bar, however, mean that we measured the loss only once due to the shortage of time and alignment trouble. Then considering the comparatively large uncertainty at a few plots, it can be explained by small difference of alignment. We sometimes had to realign all optics in the measurement at even the same target position because the lock loss happened spontaneously for some reason. Therefore it is possible that the subsequent alignment slightly deviated from the previous one and that this difference affected the loss quantities.

Information which we can obtain from the plots is the agreement of the estimated center position on both ITMX/Y. The increasing trend on both plots is consistent to some extent and the loss quantities within the off-centering of 40 [mm] remain constant, which means that the script used for estimate of the center position works very well.

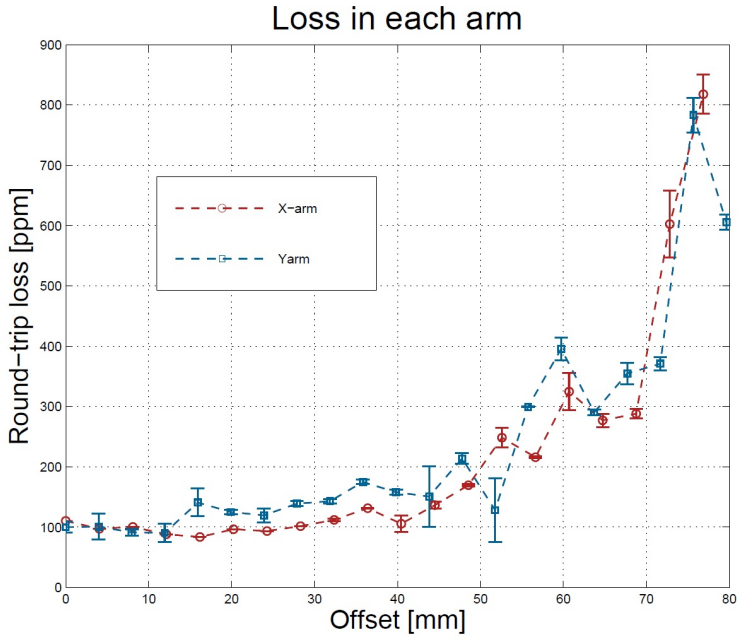

Fig 6: Data plots of the results in the both arm cavities

4.2 Evaluation of other optical quantities

As noted above, we obtained the results of not only the round trip loss but also the transmissivity of ITM, finesse and cavity mode-matching ratio. We now show these results and each standard error in TABLE.1. T_i and finesse are uniquely determined by mirrors and the component of cavities itself. Therefore we can expect them to be constant. Also WFS system adjusts mode-matching ratio to be maximum, that is, as close to 1.0 as possible. It turned out that the ringdown technique gave us greatly precise results and that the results are consistent in terms of significant precision. What we are concerned about is the confidence interval of finesse is a little higher than the reference, $417 \sim 418$, but we could not investigate this systematic error.

TABLE 1: Results of other quantities

	Finesse		T_i[%]		Mode-match ratio	
	X-arm	Y-arm	X-arm	Y-arm	X-arm	Y-arm
Mean	419.1	420.8	1.472	1.462	0.955	0.946
Std	0.7	0.5	0.004	0.003	0.005	0.004
Std/Mean[%]	0.16	0.13	0.25	0.12	0.50	0.41
95% Confidence interval	[417.7 420.5](X)		[1.468 1.480](X)		[0.945 0.965](X)	
	[419.8 421.8](Y)		[1.456 1.468](Y)		[0.938 0.950](Y)	

5 Discussion and Conclusion

5.1 Model vs Practice

We arrange the each data plots in X/Y-arm and the clipping model line together in one figure. The blue line which represents clipping model was shifted up to the loss value at the center of ITM for comparison because according to the model, clipping does not contribute to loss factors at the beam position of around the center. Fig.7 and Fig.8 show that global trend of both plot agree with the clipping model although we could not evaluate the agreement statistically because of the shortage of data plots. Additionally there are some possibilities of the reason why the results deviate from the model line at some points (e.g. around 60 [mm] on ITMX/Y and from 20 to 40 [mm] on ITMY). Firstly the actual beam position might be slightly different from the target position because the beam position sensed with the camera actually fluctuates all the time. This fluctuation seems to have significant effect on the loss result especially at points which show large optical loss. Second it is possible that only specific area scatters more beam power than other area. In any case more data plots are need to measure for more precise and statistical analysis.

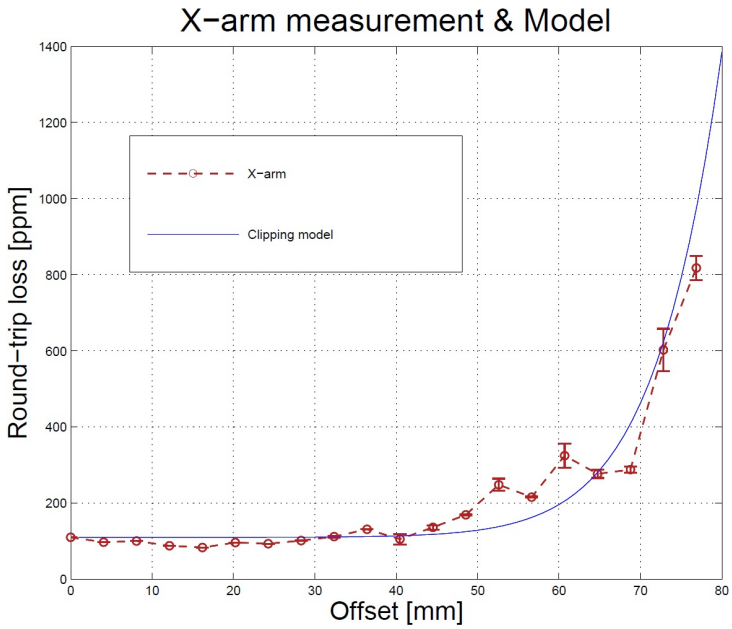

Fig 7: The results of loss in X-arm and the clipping model on the same condition

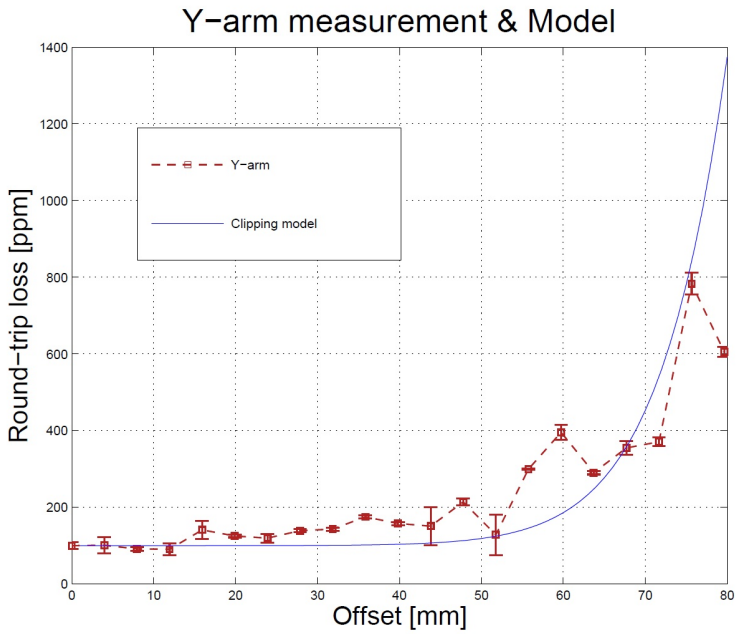

Fig 8: The results of loss in Y-arm and the clipping model on the same condition

5.2 Estimate of scattering loss

As noted in §2, we can estimate some factors other than clipping loss. Now we observe the round trip loss of around 100 [ppm] at the estimated center position in both cavities. Although some measurement already found out the scattering loss of ITMX, ETMX and ETMY to be approximately 20 [mm], 50 [mm] and 36 [mm], no reference of ITMY scattering loss is available. [5][6] Thinking about X-arm, since the scattering loss amounts to only 70 [mm], we need to investigate possible loss factors of the missing 30 [mm]. Additionally the scattering on ITMY is required to measure in order to explore multi-factors of optical loss.

5.3 Future work

This project left the three tasks to do. First of all, more sets of measurement are required at each beam position for precise analysis. Second task is to conduct the measurement not only one way but at various beam positions of the whole ITM. The 2-D loss map on ITM would be very beneficial because we could estimate the location of some point defects which would show higher scattering loss, as well as the more accurate dependence on off-centering. Lastly we need to measure overall the scattering loss on ITMY and explore other loss factor in order to explain offset quantities of the results from zero.

6 Acknowledgments

The author is extremely grateful to California Institute of Technology and LIGO livingston Laboratory for offering me the great program. Also he acknowledges the informative guidance and instruction from his supervisors, Denis Martynov and Valery Frolov, and Rana Adhikari. The measurement and data analysis were supported by the constructive discussion with Keiko Kokeyama and Hiroaki Yamamoto.

APPENDIX A

The figure below shows the components of reflected beam power which coupled beam power contributes to. Here (A), (B), (1), (2), (3) etc represent amplitude of each component field. Firstly all components can be categorized into two factors, the beam (A) which is reflected from ITM directly and the resonant beam (B) which is transmitted through ITM. (See Fig.9) (A) is written as

$$(A) = \underset{\sim\sim}{-} E_0 r_i$$

where E_0 is amplitude of the incident beam field, whose square is equal to the power of the field, that is, $P_0 = E_0 E_0^*$. (B) is given in terms of (1), (2), (3) etc as

$$(B) = t_i((1) + (2) + (3) + \cdots) = t_i \sum_{n=1}^{\infty} (n) \tag{14}$$

(1), (2) and (3) can be derived as

$$\begin{aligned} (1) &= E_0 t_i \cdot e^{-i\frac{2L}{\lambda}} r_e \\ (2) &= E_0 t_i \cdot e^{-i\frac{4L}{\lambda}} r_e \cdot r_i r_e \\ (3) &= E_0 t_i \cdot e^{-i\frac{6L}{\lambda}} r_e \cdot r_i r_e \cdot r_i r_e \end{aligned}$$

We can extrapolate to the general (n) in the same way.

$$(n) = E_0 t_i \cdot e^{-i\frac{2nL}{\lambda}} r_e \cdot (r_i r_e)^{n-1} \tag{15}$$

Thus substituting (15) for (14), (B) is represented as

$$\begin{aligned} (B) &= t_i \sum_{n=0}^{\infty} E_0 t_i r_e e^{-i\frac{2L}{\lambda}} \cdot (r_i r_e e^{-i\frac{2L}{\lambda}})^n \\ &= \frac{E_0 T_i r_e e^{-i\frac{2L}{\lambda}}}{1 - r_i r_e e^{-i\frac{2L}{\lambda}}} \end{aligned}$$

Particularly if the field is resonant in the cavity ($L = m\lambda$), we can derive $e^{-i\frac{2L}{\lambda}} = 1$. Therefore

$$\begin{aligned} (B) &= \frac{E_0 T_i r_e}{1 - r_i r_e} \\ E_{refl} &= (A) + (B) \\ &= E_0 \left(-r_i + \frac{T_i r_e}{1 - r_i r_e} \right) \end{aligned}$$

where E_{refl} is the amplitude of the reflected field from ITM. In the end the reflected power, including uncoupled factor P_1, can be written as

$$\begin{aligned} P_{refl} &= E_{refl} E_{refl}^* + P_1 = P_0 \left(-r_i + \frac{T_i r_e}{1 - r_i r_e} \right)^2 + P_1 \\ &= P_0 K [r_i - r_e (T_i + R_i)]^2 + P_1 \end{aligned}$$

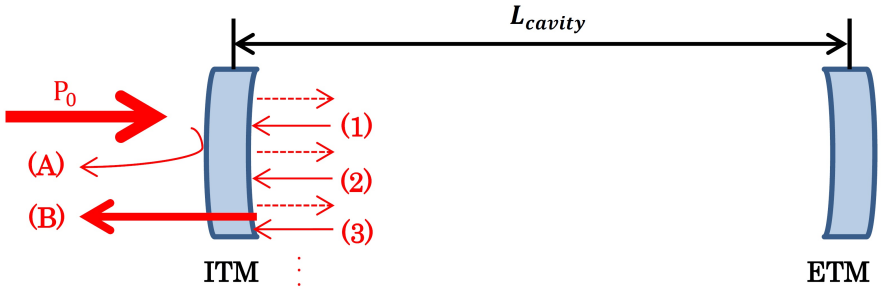

Fig 9: Components of the reflected beam power

APPENDIX B

We considered the ringdown speed of IMC as a significant factor of noise in the loss measurement. The methodology of this measurement is similar to that of the loss measurement. The only difference is to measure the transmitted power from IMC, not the reflected power. Therefore unlike Fig.4 the relaxation function does not show spike-like shape. Once the time constant, which is technically half of storage time $\tau/2$, is determined, we can derive the optical loss. As to the experimental instruments, PDA255 detector was employed to detect ringdown signal and an absorptive filter was attached with the detector's face to avoid signal saturation so that beam could travel through the filter. The transmitted power from IMC was picked off on the optical table and injected into the photo detector through the lens (focal length =143.2 [mm]) that focuses dim beam onto the detector.

Measurement

We carried out a set of measurement at totally 19th times, then fitted non-linear model function defined as $(Aexp(-t/B) + C)$ into ringdown data obtained from the oscilloscope. In the end, round-trip attenuation $(T_i + T_e + L_i + L_e)$ was derived at each measurement. Because the fluctuation of attenuation is larger than supposed quantities of losses, which are estimated by subtracting the reference $T_i + T_e$ from attenuation, some data shows negative values of optical loss. In order to avoid such an unreasonable situation, the optical loss was derived from mean of attenuations of every data.

Additionally, even this measurement requires noise reduction more or less because incident beam power does not instantly vanish in this case as well and the ringdown signal in the beginning contains some noise. As a noise reduction, we remove some data points from the beginning of ringdown up to the first-estimated value of time constant which has been computed by non-linear function regression without this correction. The values of time constant and optical loss before/after the data reduction and the ringdown waveform with fitting model in each case are shown in TABLE.2 below.

Results

The results show that despite the model function which appears to fit better after data reduction than before, the optical loss become less accurate. Actually both of the parameters before the data reduction are much closer to those calculated from the reference [2]. Although we adopted the results before the data reduction as the time constant of IMC, our method to filter out the noise is robust in any case. The reason for this discrepancy may be the unexpected vibration of ringdown waveform over the time domain of $6.5 - 7.0 \times 10^{-5}$. The cause is guessed to be the time scale of blocking beam light. We extinguished the beam power by setting the polarity switch of the MC Servo Board to be off, but it is required to explore somehow the faster method to block the incident beam.

TABLE 2: The results of loss and time constant in IMC

	Time constant [μs]	Loss [ppm]
Before data reduction	9.07	83
After data reduction	3.32	20926

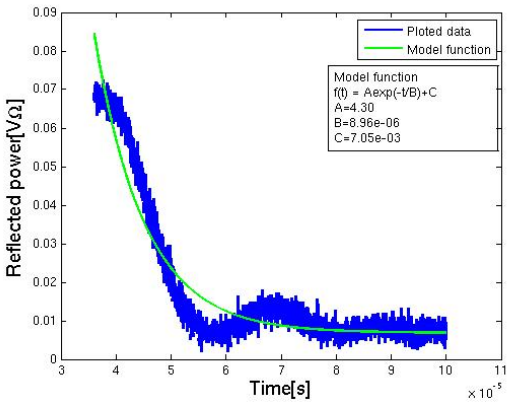

Fig 10: A sample of ringdown waveform with model function before data reduction

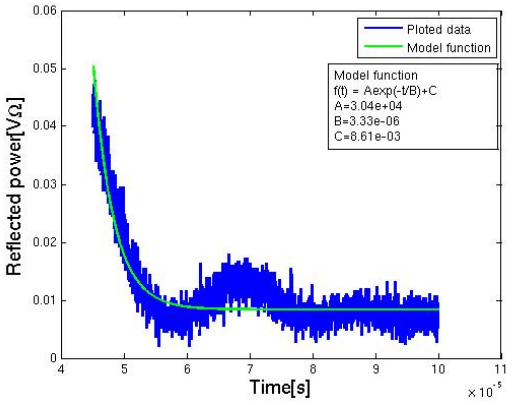

Fig 11: A sample of ringdown waveform with model function after data reduction

REFERENCE

[1] H Yamamoto, "Personal communication," 7/2 2014.

[2] P. Fritschel and E. Gustafson, "Advanced LIGO H1 Optical Layout," LIGO-D0902838-v4, Feb 2013.

[3] T Isogai, *et al.*, "Loss in long-storage-time optical cavities," LIGO-P1300159-v4, Nov 2013.

[4] B P Abbot *et al.*, "LIGO: the Laser Interferometer Gravitational-Wave Observatory," pp.6-8, 2009.

[5] J.Betzwieser, "aLIGO LLO Logbook report ID:13414," Jul 2014.

[6] D.Martynov, "aLIGO LLO Logbook report ID:11907," Apr 2014.